Water Research 167 (2019) 115106

Contents lists available at ScienceDirect

Water Research

journal homepage: www.elsevier.com/locate/watres

Integrative isotopic and molecular approach for the diagnosis and implementation of an efficient *in-situ* enhanced biological reductive dechlorination of chlorinated ethenes

Natàlia Blázquez-Pallí [a, b], Mònica Rosell [c], Joan Varias [b], Marçal Bosch [b], Albert Soler [c], Teresa Vicent [a], Ernest Marco-Urrea [a, *]

[a] Departament d'Enginyeria Química, Biològica i Ambiental, Universitat Autònoma de Barcelona (UAB), c/ de les Sitges s/n, 08193, Cerdanyola del Vallès, Spain
[b] Litoclean, S.L, c/ Numància 36, 08029, Barcelona, Spain
[c] Grup MAiMA, SGR Mineralogia Aplicada, Geoquímica i Geomicrobiologia, Departament de Mineralogia, Petrologia i Geologia Aplicada, Facultat de Ciències de la Terra, Institut de Recerca de l'Aigua (IdRA), Universitat de Barcelona (UB), c/ Martí Franquès s/n, 08028, Barcelona, Spain

ARTICLE INFO

Article history:
Received 3 July 2019
Received in revised form
18 September 2019
Accepted 21 September 2019
Available online 23 September 2019

Keywords:
Chlorinated ethenes
Organohalide-respiring bacteria
Dehalococcoides
In-situ pilot test
Enhanced reductive dechlorination
Carbon isotopic mass balance

ABSTRACT

Based on the previously observed intrinsic bioremediation potential of a site originally contaminated with perchloroethene (PCE), field-derived lactate-amended microcosms were performed to test different lactate isomers and concentrations, and find clearer isotopic and molecular parameters proving the feasibility of an *in-situ* enhanced reductive dechlorination (ERD) from PCE-to-ethene (ETH). According to these laboratory results, which confirmed the presence of *Dehalococcoides* sp. and the *vcrA* gene, an *in-situ* ERD pilot test consisting of a single injection of lactate in a monitoring well was performed and monitored for 190 days. The parameters used to follow the performance of the ERD comprised the analysis of i) hydrochemistry, including redox potential (Eh), and the concentrations of redox sensitive species, chlorinated ethenes (CEs), lactate, and acetate; ii) stable isotope composition of carbon of CEs, and sulphur and oxygen of sulphate; and iii) 16S rRNA gene sequencing from groundwater samples. Thus, it was proved that the injection of lactate promoted sulphate-reducing conditions, with the subsequent decrease in Eh, which allowed for the full reductive dechlorination of PCE to ETH in the injection well. The biodegradation of CEs was also confirmed by the enrichment in ^{13}C and carbon isotopic mass balances. The metagenomic results evidenced the shift in the composition of the microbial population towards the predominance of fermentative bacteria. Given the success of the *in-situ* pilot test, a full-scale ERD with lactate was then implemented at the site. After one year of treatment, PCE and trichloroethene were mostly depleted, whereas vinyl chloride (VC) and ETH were the predominant metabolites. Most importantly, the shift of the carbon isotopic mass balances towards more positive values confirmed the complete reductive dechlorination, including the VC-to-ETH reaction step. The combination of techniques used here provides complementary lines of evidence for the diagnosis of the intrinsic biodegradation potential of a polluted site, but also to monitor the progress, identify potential difficulties, and evaluate the success of ERD at the field scale.

1. Introduction

Chlorinated ethenes (CEs) are among the most ubiquitous anthropogenic groundwater contaminants due to their widespread use in industry and recalcitrance under oxic conditions. CEs are considered priority substances (ATSDR, 2017) and have maximum contaminant levels in groundwater set by the 2008/105/EC European Directive (European Commission, 2008). Perchloroethene (PCE) is resistant to aerobic degradation but under anoxic conditions can undergo reductive dechlorination to the less-chlorinated ethenes trichloroethene (TCE), *cis*- and *trans*-dichloroethene (*cis*-, *trans*-DCE), vinyl chloride (VC), and the harmless end-product ethene (ETH).

Organohalide-respiring bacteria (OHRB) provide a potential

* Corresponding author.
E-mail address: ernest.marco@uab.cat (E. Marco-Urrea).

https://doi.org/10.1016/j.watres.2019.115106
0043-1354/

solution to detoxify sites impacted with CEs due to their capability to use organochlorides as electron acceptors to support their growth, which result in a stepwise reduction of CEs (Bradley, 2000; Leys et al., 2013). Several OHRB can partially dechlorinate PCE to TCE or *cis*-DCE, e.g. *Geobacter* sp., but *Dehalococcoides* sp. (*Dhc*) and *Dehalogenimonas* sp. are the only genera, to date, capable of fully dechlorinating CEs to ETH (Adrian and Löffler, 2016; Yang et al., 2017b). Reductive dehalogenases (*rdh*) are the key enzymes driving organohalide respiration and can be used as biomarkers to investigate the intrinsic bioremediation potential at polluted sites (Blázquez-Pallí et al., 2019; Dugat-Bony et al., 2012; Hermon et al., 2019; Scheutz et al., 2008). Compound-specific stable isotope analysis (CSIA) can provide a complementary line of evidence to monitor biodegradation of chlorinated compounds in groundwater (Aelion et al., 2009; Hermon et al., 2018; Hunkeler et al., 1999; Nijenhuis et al., 2007; Palau et al., 2014). This technique measures a specific stable isotope ratio (e.g. $^{13}C/^{12}C$) within molecules and is based on light and heavy isotopes degrading at slightly different rates during biochemical transformations. Such shift in the isotopic composition (δ) of the molecule can be used to confirm and quantify *in-situ* biodegradation and distinguish degradation pathways (Elsner, 2010). This is possible because the isotopic enrichment caused by physical processes such as volatilization, sorption, or dilution, is considered to be negligible (Aelion et al., 2009; Hunkeler et al., 1999). Similarly, the isotopic composition of certain non-halogenated potential electron acceptors can be used to trace changes in the redox potential of the groundwater. For instance, a dual isotope approach can be used to measure the extent of sulphate reduction because this reaction results in an enrichment in both ^{34}S and ^{18}O in the residual sulphate (Wu et al., 2011).

When OHRB are present but the electron donor becomes a limiting factor, the groundwater contaminated with CEs can show little to no dechlorination past *cis*-DCE, resulting in the accumulation of toxic intermediates (DCE or VC stall) (Bradley, 2000; Stroo and Ward, 2010). To avoid this, groundwater can be conditioned with organic fermentable substrates (e.g. lactate), which can generate reducing equivalents that promote the sequential dechlorination to ETH. This bioremediation approach is commonly referred to as biostimulation or ERD, which stands for enhanced reductive dechlorination (Adrian and Löffler, 2016; Leeson et al., 2004). To date, many studies have focused on laboratory methodologies to assess and characterize the intrinsic bioremediation potential of CEs-polluted sites by OHRB (Buchner et al., 2015; Courbet et al., 2011; Ebert et al., 2010; Kuder et al., 2013; Lee et al., 2016; Lu et al., 2009; Matteucci et al., 2015; Nijenhuis et al., 2007; Slater et al., 2001; Tarnawski et al., 2016; Yu et al., 2018), but few have reported results after applying ERD and CSIA at the field scale (Herrero et al., 2019; Hirschorn et al., 2007; Song et al., 2002).

The research reported in Blázquez-Pallí et al. (2019) presented a multi-method approach to assess the intrinsic biodegradation potential of an industrial site in Barcelona (Spain) polluted by CEs. Obtained results discouraged natural attenuation as a remediation strategy due to *cis*-DCE stall, and recommended an ERD injecting lactate as electron donor. In line with those conclusions, the present study aimed at continuing the remediation work at that same aquifer and apply an integrated isotopic and molecular approach that provides complementary lines of evidence to implement, monitor and assess an efficient *in-situ* biodegradation of CEs at the site during an ERD. To this end, a more detailed laboratory study focusing, as well, on the concentration and isomeric form of lactate required for the complete dechlorination of PCE to ETH was performed first, followed by the monitoring of the *in-situ* ERD pilot test and the final full-scale treatment. The used methodology in all cases combined (1) the acquisition of hydrogeochemical data, (2) microcosms experiments, (3) molecular techniques (i.e. identification of selected biomarkers and 16S rRNA high-throughput sequencing of groundwater samples), and (4) stable isotopes of sulphate (as model redox sensitive species), and carbon from the target contaminants (CEs).

2. Materials and methods

2.1. Chemicals

PCE (99.9% purity) was from Panreac; laboratory-grade sodium DL-lactate (≥98% purity) from Sigma-Aldrich (hereinafter, Lactate-1), and food-grade sodium L-lactate (97% purity, at 60% w/w) from Purac (Corbion) (hereinafter, Lactate-2). Other chemicals and reagents used for the present study were purchased from Sigma-Aldrich, Thermofisher and Bio-Rad at scientific grade or higher.

2.2. Study site

The studied site is located in the Barcelona province (Spain) and the aquifer is mainly constituted by three lithological units: i) a lower layer of reddish clay loams, ii) an intermediate layer of brown and silty clays, and iii) an upper layer of ochre silty clays. Given such lithology, the hydraulic conductivity is generally low, only improved by localized gravel and sandstone areas that increase the permeability of the media and could act as preferential flow paths. A hydrogeological cross section of the site is depicted in Figs. S1 and a more detailed description of the aquifer can be found elsewhere (Blázquez-Pallí et al., 2019). A preliminary site characterization revealed a significant PCE plume, accompanied by minor amounts of TCE, *cis*-DCE and VC. Originally, it was treated by a combination of pump and treat (P&T) and dual-phase extraction (DPE, vapour and groundwater). Pumped groundwater was later treated through an air stripping system. Groundwater flowed naturally in the NW–SE direction (Fig. 1); however, under such ongoing remediation, all the extraction points were almost dried due to the low productivity of the aquifer. These P&T and DPE systems were halted partially during the *in-situ* pilot test (only remained active in some wells outside the pilot test area), and completely for the full-scale bioremediation. However, certain influence of this pumping on the groundwater flow direction during the *in-situ* pilot test cannot be discarded.

2.3. Microcosm experiments

Groundwater with fine sediments was collected from the intended pilot scale injection well PZ-2 (Fig. 1) with a peristaltic pump on October 4th, 2016, in transparent sterile glass bottles that were sealed with PTFE caps as described elsewhere (Blázquez-Pallí et al., 2019). These groundwater samples were kept in the dark at 4 °C until the following day, when microcosms were set up. Four different treatments were prepared, at least in duplicate: (1) control containing only groundwater, (2) groundwater with Lactate-1 at ~ 3 mM, (3) groundwater with Lactate-2 at ~ 3 mM, and (4) groundwater with Lactate-2 at ~ 15 mM. Each 100 mL microcosm bottle contained 65 mL of sampled groundwater with fine sediments and the lactate concentrations described above. All microcosms were prepared in an anoxic glovebox and incubated in the dark at 25 °C. Microcosms that fully dechlorinated CEs were reamended with TCE and transferred to sterilized anoxic synthetic medium (3–7% v/v) described elsewhere (Martín-González et al., 2015) during the exponential degradation phase of CEs.

For the analysis of the site-specific carbon isotopic fractionation (εC) during degradation of PCE, six parallel anoxic cultures were prepared with the abovementioned defined medium and groundwater from PZ-2 (1.5% v/v) as inoculum. Each culture was spiked

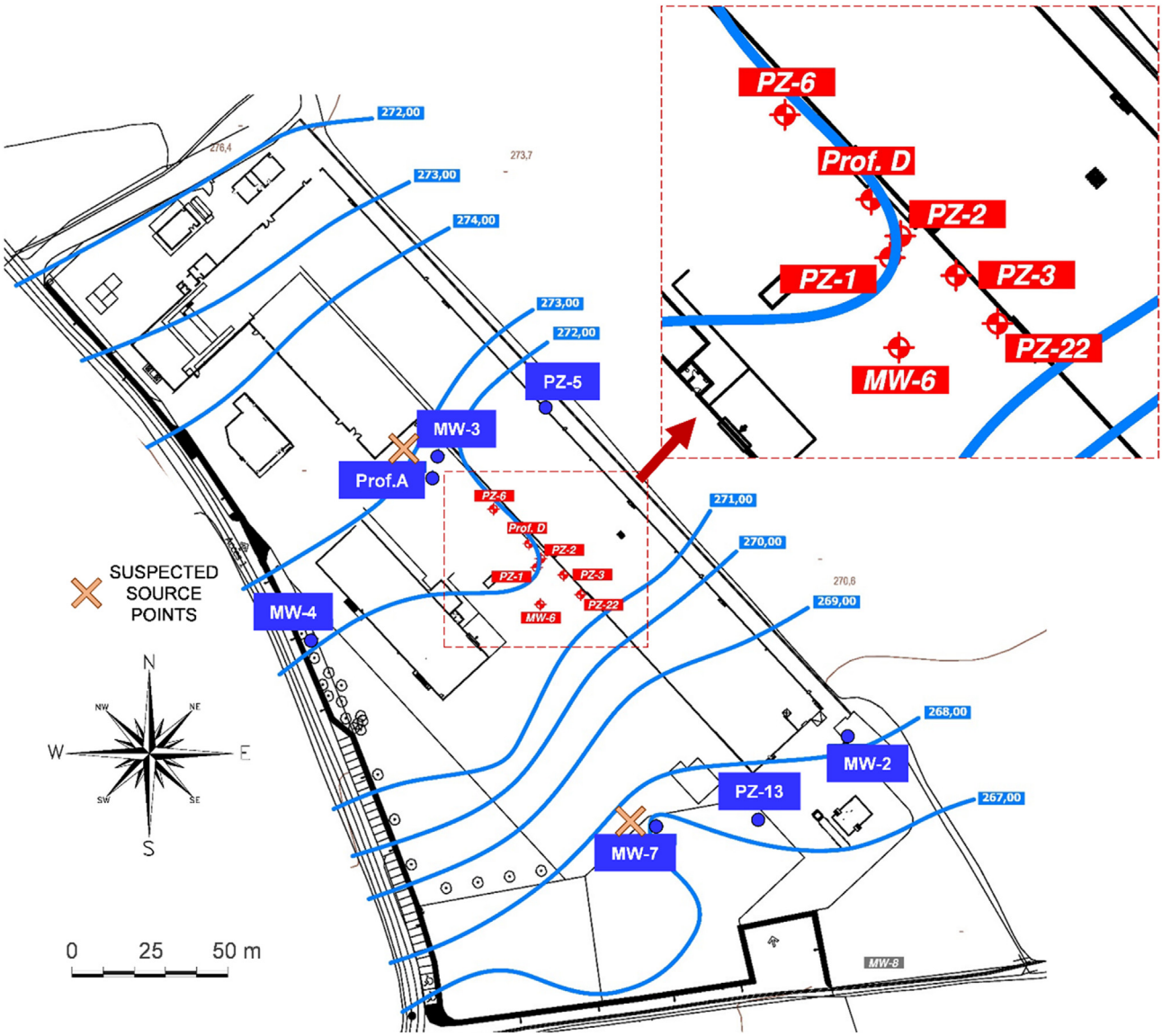

Fig. 1. Water table (blue lines, in m.a.s.l.) representative of the natural groundwater flow at the site and location of monitoring wells. Red numerical codes refer to the wells monitored during the *in-situ* ERD pilot test. (For interpretation of the references to colour in this figure legend, the reader is referred to the Web version of this article.)

with PCE (235 μM), and sacrificed with NaOH (10 M) at 0, 1, 6, 77, 88, 96 and 97% of PCE degradation. Three different controls were prepared in duplicate: (1) killed controls with PCE, (2) killed controls without PCE, and (3) abiotic controls with PCE.

2.4. Implementation of the ERD in-situ pilot test

The pilot test consisted of a unique injection of lactate at well PZ-2 (Fig. 1) on October 25th, 2016 (t_0). The product injected was an aqueous solution of Lactate-2 diluted with groundwater outflowing from the air stripping system installed at the site. The total volume of substrate injected was lower than 10% of the treatment zone volume. The design parameters of the *in-situ* pilot test were based on the recommendations from Leeson et al. (2004) and Dugat-Bony et al. (2012).

2.5. Monitoring of the ERD in-situ pilot test

Field parameters (i.e. Eh, pH, T, and electric conductivity (EC)) were measured *in-situ* and groundwater was collected with a peristaltic pump from the injection well PZ-2 and nearby wells PZ-1, PZ-3, PZ-6, PZ-22, MW-6, and Prof.D (Fig. 1) as described elsewhere (Blázquez-Pallí et al., 2019). Sampling campaigns were carried out the day before injection of lactate (t_{-1}, October 24th, 2016) and the next 2, 9, 20, 50, 86, 142 and 190 days after the injection (hereinafter, t_i). Samples collected for both CSIA and CEs concentration were immediately killed with NaOH (pH > 10) and stored at 4 °C until analysed. Short-chain volatile fatty acids (VFAs) were analysed from groundwater samples filtered on site (0.20 μm) and stored in borosilicate tubes at 4 °C until analysed.

2.6. Isotopic evaluation of the full-scale ERD treatment

A full-scale ERD treatment was implemented by Litoclean, S.L. on August 2017. The bioremediation strategy consisted in the injection of Lactate-2 every three months for the period of a year. Between 30 and 50 out of a total of 66 monitoring wells at the site were used for the injection of the substrate at every event but

changing the distribution of the injections to ensure the maximum coverage of the plume area. On September 2018, after one year of treatment, groundwater was sampled from wells PZ-3, PZ-5, PZ-22, MW-3, MW-6, and MW-7 (Fig. 1) following the same methodology mentioned in section 2.5. Samples were analysed for CEs concentrations and CSIA, and data were compared to previous (before the *in-situ* pilot test) chemical and isotopic values for each well.

2.7. Analytical methods

CEs concentrations were analysed from 500 μL headspace samples by gas chromatography (GC) coupled to a flame ionization detector (FID) as reported by Martín-González et al. (2015). VFAs (lactate, pyruvate, acetate, formate) were analysed by high performance liquid chromatography (HPLC) from filtered liquid samples as described elsewhere (Mortan et al., 2017).

Stable carbon isotopes of CEs were analysed with an Agilent 6890 GC coupled to an IRMS at *Centres Científics i Tecnològics de la Universitat de Barcelona* (CCiT-UB), following the procedure described in Blázquez-Pallí et al. (2019). Carbon isotopic compositions in all samples are presented in delta notation ($\delta^{13}C$, in ‰), relative to the international standard Vienna Pee Dee Belemnite (VPDB), following

$$\delta^{13}C = \left(\frac{R_{sample}}{R_{std}} - 1\right) \cdot 1000 \quad (1)$$

where R_{sample} and R_{std} represent the isotope ratios (e.g. $^{13}C/^{12}C$) of the sample and the standard, respectively (Elsner, 2010). Instrument uncertainty was considered as the standard deviation (1σ) of duplicate measurements. For field data, the degradation is considered significant if the shift in $\delta^{13}C$ is > 2‰ compared to its original value (Hunkeler et al., 2008).

Carbon isotopic mass balance for CEs at each monitoring well was calculated according to Aeppli et al. (2010) and Hunkeler et al. (1999), as follows

$$\delta^{13}C_{sum} = x_{PCE} \cdot \delta^{13}C_{PCE} + x_{TCE} \cdot \delta^{13}C_{TCE} + x_{DCE} \cdot \delta^{13}C_{DCE} + x_{VC} \cdot \delta^{13}C_{VC} \quad (2)$$

where *x* is the molar fraction of each substance with respect to the total molar mass (sum of CEs for which $\delta^{13}C$ values were available) for each sample at each sampling event. In this case, as PCE was the only contaminant spilled in this aquifer, the $\delta^{13}C_{sum}$ must remain constant as long as (1) PCE released along the time and space had the same isotopic composition, (2) the unique transformation pathway was reductive dechlorination, (3) VC does not further degrade to ETH when considered in the balance (Aeppli et al., 2010; Hunkeler et al., 1999; Palau et al., 2014).

The logarithmic form of the simplified Rayleigh equation correlates changes in the carbon isotope ratios (R_t/R_0) and changes in concentrations ($f = C_t/C_0$) with time for a closed system (Elsner, 2010), and the obtained epsilon (εC) represents the carbon isotopic fractionation, as follows

$$ln\left(\frac{R_t}{R_0}\right) = \varepsilon C \cdot ln(f) \quad (3)$$

where R_t/R_0 can be expressed as $(\delta^{13}C_t + 1)/(\delta^{13}C_0 + 1)$.

The analysis of major anions (HCO_3^-, NO_3^-, Cl^-, SO_4^{-2}) and cations (Na^+, K^+, Ca^{+2}, Mg^{+2}) was performed at CCiT-UB. Total concentrations of Na^+, K^+, Ca^{+2}, Mg^{+2} were analysed by inductively coupled plasma-optic emission spectrometry (ICP-OES, Optima 3200 RL) and by inductively coupled plasma mass spectrometry (ICP-MS, Elan 6000). NO_3^-, Cl^-, and SO_4^{-2} concentrations were determined by HPLC using a WATERS 515 HPLC pump with an IC-PAC anion column and a WATERS detector (mod 432), while HCO_3^- was measured by titration (METROHM 702SM Titrino). The predominant equilibrium systems controlling the Eh were investigated via Eh−pH predominance diagrams prepared with the MEDUSA code (Puigdomènech, 2010).

Dissolved SO_4^{-2} detected in groundwater was precipitated as $BaSO_4$ as reported elsewhere (Dogramaci et al., 2001) and its sulphur and oxygen isotopic compositions were analysed following Rodríguez-Fernández et al. (2018). Results are presented in delta notation ($\delta^{34}S-SO_4^{-2}$ and $\delta^{18}O-SO_4^{-2}$, in ‰), relative to the international standards, Vienna Standard Mean Oceanic Water (VSMOW) for $\delta^{18}O$ and Vienna Canyon Diablo Troillite (VCDT) for $\delta^{34}S$.

2.8. DNA extraction, PCR and 16S rRNA gene high-throughput sequencing

DNA for molecular analyses was extracted from TCE-enriched field-derived cultures (three transfers into fresh synthetic medium) that were originally amended with Lactate-2 (~3 mM) and from well PZ-2. Cell harvesting, genomic DNA isolation and PCR reaction for amplification of the *vcrA* gene were performed as described in Blázquez-Pallí et al. (2019). Primer sets used are detailed in Table S1.

To investigate the OHRB involved in the biodegradation of CEs to ETH, the dilution-to-extinction method (Löffler et al., 2005) was applied in 20-mL vials containing 12 mL of the anoxic synthetic medium mentioned in section 2.3, but using 1 mL of active TCE-enriched field-derived culture as inoculum and *cis*-DCE as electron acceptor. After three extinction series, the more diluted vial showing ETH formation was used as inoculum for serum bottle microcosms and, after consuming 10 μM *cis*-DCE, was selected for 16S rRNA analysis. After DNA extraction, amplicons of the region V3−V4 for 16S rRNA genes were amplified with primers S-D-Bact-0341-b-S-17 and S-D-Bact-0785-a-A-21 (Klindworth et al., 2013) with the Illumina MiSeq sequencing platform at *Serveis de Genòmica i Bioinformàtica* from *Universitat Autònoma de Barcelona* (Spain).

To characterize the impact of the injection of lactate on the bacterial community structure after the *in-situ* pilot test, 80 mL of groundwater were collected from wells PZ-2, PZ-1, and PZ-22 at t_{-1} and t_{142}. Samples were stored at −20 °C until DNA extraction and 16S rRNA gene high-throughput sequencing were performed at All Genetics & Biology (A Coruña, Spain). For DNA extraction, samples were centrifuged at 5000 *g* for 1 h and the pellet was transferred to PowerBead tubes of the DNeasy Powersoil DNA isolation kit (Qiagen). DNA was isolated following the instructions of the manufacturer. For library preparation, a fragment of the bacterial 16S rRNA region of around 450 bp was amplified using primers Bakt_341F and Bakt_805R (Herlemann et al., 2011). The pool was sequenced in a MiSeq PE300 run (Illumina).

3. Results and discussion

3.1. Feasibility and markers for complete ERD at laboratory scale

3.1.1. Assessment of the lactate isomers and concentration in microcosm experiments

Microcosms were prepared to test whether reductive dechlorination of CEs to ETH was feasible in the injection well PZ-2. Besides the control, which accounted for monitored natural attenuation (MNA), two different isomeric forms of sodium lactate (DL-/Lactate-1 and L-/Lactate-2) were used to test their effect on the

lactate fermentation potential of the native microbial community. Moreover, Lactate-2 was used because it was a candidate product in a foreseeable *in-situ* pilot test. Accordingly, Lactate-2 was amended at two different concentrations to discard inhibition effects. On the one hand, the unamended controls transformed PCE to *cis*-DCE and VC within 15 days, but ETH was not detected. When microcosms were reamended with TCE (35 μM) at day 25, dechlorination barely passed VC, and ETH was detected at low concentration after 50 days (Fig. S2A). On the other hand, lactate-amended treatments fully dechlorinated PCE to ETH within 15 days and exhibited similar rates independently of the isomeric form and concentration (Fig. S2, B–D). After adding TCE in all three of them at days 25 and 45, the dechlorination remained active with the consequent accumulation of ETH (Fig. S2, B–D). In all amended microcosms, lactate was totally consumed and acetate was produced within 10 days (data not shown). However, excess of electron donor and, thus, of H_2, did promote methanogenesis, resulting in a vigorous formation of methane in the microcosm with ~15 mM of lactate (Fig. S3), which has been reported before (Blázquez-Pallí et al., 2019; Leeson et al., 2004).

3.1.2. Identification of vcrA gene and CEs dechlorinating bacteria

PCR amplifications with the *vcrA* gene-targeted primer were run to investigate whether the *vcrA* gene was present in the TCE-enriched field-derived cultures from well PZ-2 (section 2.8). After gel electrophoresis, observed diagnostic amplicons indicated that the culture contained *vcrA* gene, which is implicated in the VC-to-ETH dechlorination step (Fig. S4).

In these TCE-enriched cultures, three dilution-to-extinction series were applied using *cis*-DCE as electron acceptor to get insight into the OHRB responsible for ETH generation. The 16S rRNA gene amplicon sequencing and the taxonomic assignments revealed that the four predominant genera were *Pleomorphomonas* (50%), described as nitrogen-fixing bacteria (Im et al., 2006; Madhaiyan et al., 2013; Xie and Yokota, 2005); *Desulfomicrobium* (18%), which are sulphate-reducing bacteria (Sharak Genthner et al., 1997, 1994); and the OHRB *Geobacter* (14%) and *Dehalococcoides* (3%) (Fig. 2). *Geobacter* sp. can derive energy from acetate oxidation coupled to PCE-to-*cis*-DCE dechlorination, but it is also capable of growing on a wide range of non-halogenated electron acceptors (Atashgahi et al., 2016; Sanford et al., 2016). The presence of *Dehalococcoides* was consistent with the detection of *vcrA* reductive dehalogenase gene (Fig. S4) and ETH generation in lactate-amended microcosms (Fig. S2).

3.1.3. Site-specific εC for PCE degradation

The analysis of site-specific εC can help estimate the extent of the *in-situ* biodegradation of contaminants in the field (Elsner, 2010). PCE was depleted in the microcosms inoculated with groundwater from PZ-2 (Fig. S5A) but dechlorination was not accompanied by a significant change in its isotopic composition ($\delta^{13}C_{PCE}$) (Fig. S5B). In more detail, $\delta^{13}C_{PCE}$ shifted only 0.81‰ and 1σ for duplicate measurements were, for all samples, below total instrumental uncertainty of 0.5‰ (Sherwood Lollar et al., 2007). The dechlorination reaction did not fit the Rayleigh model (Eq. (3), $R^2 = 0.63$, $\varepsilon C = -0.2 \pm 0.2$‰), which deemed this site-specific εC as not significant (ns). In contrast, a stronger enrichment in ^{13}C was observed when the produced TCE was further degraded to *cis*-DCE (Fig. S5B). This non-linear εC for PCE is, most likely, the combined effect of several OHRB simultaneously transforming PCE, with a major contribution of the non-fractionating species. This agrees with the predominance of *Geobacter* sp. in the cultures (Fig. 2), which is reported to have a non-significant εC for PCE and could have lead the PCE-to-TCE dechlorination (Table S2) (Cichocka et al., 2008). Abiotic and NaOH-killed controls did not show PCE losses or degradation as its concentration did not vary significantly throughout the whole experiment (236 ± 8 μM, n = 6, Fig. S5A) and no degradation products were detected.

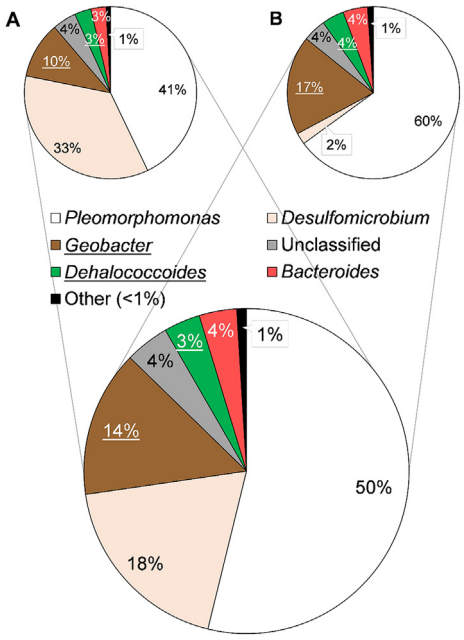

Fig. 2. Microbial population in enriched cultures derived from microcosms amended with Lactate-2 from well PZ-2. Average composition obtained from two cultures (A and B) that were enriched with TCE first, and later with *cis*-DCE for several consecutive dilution series. Total sequence reads for the genera *Geobacter* and *Dehalococcoides* were, respectively, 24232/140088 and 5393/140088 in replicate A, and 10421/103805 and 3023/103805 in replicate B. Genera with abundance <1% are grouped in "Other".

3.2. In-situ ERD pilot test with lactate at the injection well PZ-2

Microcosms of PZ-2, which mimicked the natural attenuation conditions at the site, indicated that reductive dechlorination could stall at an intermediate stage, resulting in an accumulation of *cis*-DCE and VC (Fig. S2A). However, the amendment of lactate resulted in a faster dechlorination of PCE and concomitant generation of ETH (Fig. S2, B–D). Considering these results, an *in-situ* ERD pilot test with Lactate-2 was implemented at well PZ-2.

3.2.1. Hydrochemistry changes induced by the lactate injection

The concentration of major anions (SO_4^{-2}, NO_3^-, HCO_3^-, Cl^-) and cations (Na^+, K^+, Ca^{+2}, Mg^{+2}) was analysed at t_{-1}, t_{20}, t_{86} and t_{190}. At the injection well PZ-2, NO_3^- and SO_4^{-2} were depleted after the addition of the Lactate-2 solution (Fig. S6A), whereas Na^+, Ca^{+2}, Mg^{+2} and electric conductivity (EC) increased, responding to the injected electron donor (Table S3). At the monitoring wells PZ-1, PZ-6 and MW-6, NO_3^- concentrations were depleted as well, but different trends were observed for SO_4^{-2} (Figure S6, A and B). In contrast, no significant changes were observed for those anions in monitoring wells PZ-3, PZ-22, and Prof.D (Fig. S6C).

Geochemical modelling shows that the aquifer was at nitrate-reducing conditions before injection and that the addition of lactate promoted a shift towards sulphate-reducing and methanogenic conditions (Fig. S7). This shift was more extreme in the injection well PZ-2 (at t_{20}) as well as in monitoring wells PZ-1 (at t_{86}), and PZ-6 and MW-6 (both at t_{190}), which agrees with the decrease observed in NO_3^- and SO_4^{-2} concentrations (Fig. S6). In addition, results suggested that the system was controlled by calcite ($CaCO_3(s)$) (Fig. S7B), as the pH was maintained within the

range of 6–8, the optimal for OHRB (Yang et al., 2017a).

$\delta^{34}S$ and $\delta^{18}O$ values of dissolved SO_4^{-2} from t_{-1} at each monitoring well were compared with the ones obtained after the lactate injection (t_{20}, t_{86} or t_{190}). Before the injection, the S and O isotopic composition of SO_4^{-2} at the site showed diverse values corresponding to a mixture among geogenic composition (Triassic or Tertiary recycled gypsum) in well Prof.D, synthetic fertilizers, and an unknown source (with the lowest ^{34}S and ^{18}O values) that could be related to agricultural uses of manure (Otero et al., 2008). This variability points out to a heterogeneity in the origin of the dissolved sulphate in the aquifer (Fig. 3). In any case, in the injection well PZ-2, isotopic compositions at t_{20} became significantly more enriched with a shift of $\Delta\delta^{34}S = +3.0‰$ and $\Delta\delta^{18}O = +3.2‰$ resulting in a slope of 1.1 (Fig. 3). These $\delta^{34}S$ and $\delta^{18}O$ values of sulphate seem influenced by the mixing with the sulphate isotopic composition of the injected water (Fig. 3). Unluckily, no values could be obtained for t_{86} or t_{190} due to concentrations being below the limit of quantification. An even larger shift was measured in monitoring wells PZ-6 and MW-6 because the slower decrease of SO_4^{-2} concentrations allowed the measurement of more points. By t_{190}, PZ-6 showed the most ^{34}S enriched value measured at the site, also with respect to its t_{-1} ($\Delta\delta^{34}S = +14.4‰$), but with a small $\delta^{18}O$ enrichment ($\Delta\delta^{18}O = +1.0‰$) (Fig. 3). For MW-6, the most enriched $\delta^{34}S$ was measured in t_{86} ($\Delta\delta^{34}S = +7.4‰$), while the largest $\Delta\delta^{18}O$, of +4.7‰, was measured in t_{190} (Fig. 3). In contrast, $\Delta\delta^{34}S$ and $\Delta\delta^{18}O$ in monitoring wells PZ-1, PZ-3, PZ-22, and Prof.D were not significant (Fig. 3). A wide variation in the dual S–O slopes have been described for bacterial sulphate reduction in different natural environments (from 0.23 to 1.7) (Antler et al., 2013; Mizutani and Rafter, 1973). These differences have been linked to the net sulphate reduction rate and to the recycling of intermediate species (such as sulphite that facilitate oxygen isotope exchange with H_2O) back to sulphate. In environments where sulphate reduction is fast, this sulphite re-oxidation is minimal resulting in lower slopes due to sulphur isotopes increasing faster than oxygen isotopes (Antler et al., 2013). Thus, obtained results (with the available data points) proved sulphate reduction after lactate injection only in PZ-6 and MW-6 by isotopic enrichment rather than pure mixing with injected water.

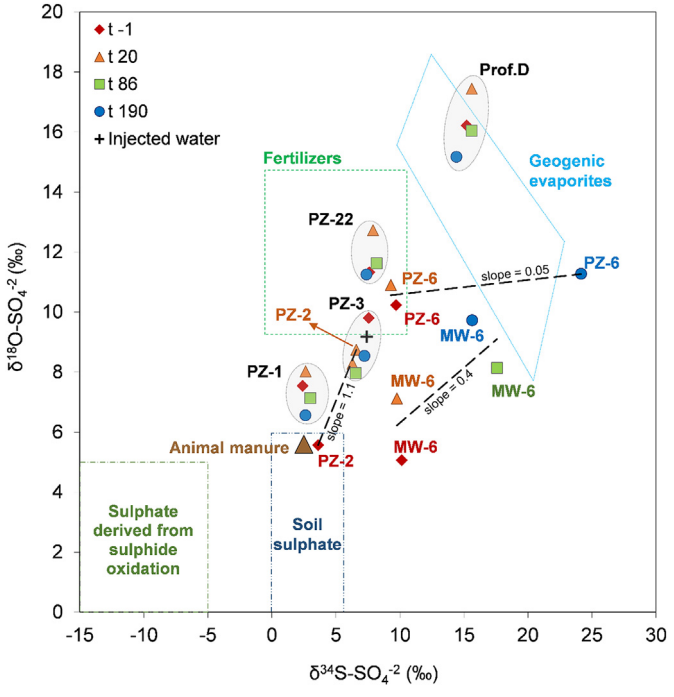

Fig. 3. Dual S–O isotopic compositions of SO_4^{-2} during the *in-situ* ERD pilot test in all monitored wells. "Injected water" refers to the groundwater collected from across the aquifer, treated through an air stripping system, later mixed with Lactate-2, and injected into well PZ-2 for the pilot test. Samples t_{86} and t_{190} for PZ-2 had too low SO_4^{-2} concentration for isotopic measurements, while sample t_{86} for PZ-6 was lost. Dashed black lines represent the slopes estimated for each well with the available values. Shapes of symbols indicate different sampling events, while colours indicate different monitoring wells. (For interpretation of the references to colour in this figure legend, the reader is referred to the Web version of this article.)

3.2.2. Enhanced biodegradation of chlorinated ethenes at the injection well PZ-2

PCE was the main toxic substance dissolved in groundwater of PZ-2 before lactate injection (Fig. 4A). After biostimulation, Eh decreased from +300 to 400 mV to ~ −50 mV by t_{20} (Fig. 4D) and acetate was detected for the first time by t_{50} (Fig. 4C). The generation of reducing equivalents from lactate fermentation and the subsequent dramatic decrease of Eh favoured dechlorination past *cis*-DCE and VC up to ETH by t_{190} (Fig. 4A). The full dechlorination of CEs to ETH by t_{190} was also confirmed by the enrichment in the isotopic mass balance ($\delta^{13}C_{sum}$), which changed from $-33 \pm 2‰$ to $-9.0 \pm 0.5‰$ (Fig. 4B). This difference in the $\delta^{13}C_{sum}$ is due to not considering the isotopic composition of ETH after VC degradation (which would be depleted as lighter isotopes react faster). Hence, $\delta^{13}C_{sum}$ became less negative as VC to ETH reaction progressed. In detail, the PCE to TCE reaction at PZ-2 did not change $\delta^{13}C_{PCE}$ significantly and remained constant throughout the whole monitoring period (Fig. 4B), emulating the results of the microcosm experiments ($\varepsilon C = ns$) (section 3.1.3.). Conversely, TCE and *cis*-DCE showed variations in $\delta^{13}C$ during the *in-situ* dechlorination process, which were up to +7‰ for TCE and +16‰ for *cis*-DCE at the measured times (Fig. 4B). Lastly, VC could be nicely traced, exhibiting a remarkable variation of $\delta^{13}C$ (shift up to +49‰) including its formation from *cis*-DCE and degradation to ETH by t_{190} (Fig. 4B).

3.2.3. Impact of the in-situ ERD pilot test at wells within the direct radius of influence

Lactate and/or acetate were progressively detected in PZ-1 (at t_2), PZ-6 (at t_{20}) and finally in MW-6 (at t_{142}), indicating the arrival of the injected solution through the preferential groundwater flow paths (with a stronger N–S direction than at natural conditions, Fig. 1), thus drawing the direct radius of influence of the *in-situ* ERD pilot test. Another evidence of the affectation at these wells was the dramatic decrease in Eh like the one observed in the injection well PZ-2 (Figs. S8, S9, S10). However, even when reaching similar negative Eh values (down to −100 mV), the PCE reductive dechlorination mainly stalled at *cis*-DCE (most evident in PZ-1) (Figs. 5, S8, S9, S10), while in PZ-6 (farther from PZ-2) *cis*-DCE started to pass to VC and ETH by t_{190} (Fig. S9A). These concentration data agree with $\delta^{13}C_{sum}$ of CEs remaining constant in the three wells (~−32‰ over 190 days, Figs. 5, S8B, S9B, S10B), so there was no significant alternative degradation pathways besides ERD, and ETH generation was still minor compared to PZ-2. Curiously, the most inefficient ERD (*cis*-DCE stall confirmed by no changes in its $\delta^{13}C_{cis\text{-}DCE}$ after t_{50}) of these wells occurred in PZ-1, where the initial drop in the Eh was followed by a rebound to more positive values after t_{86} (Fig. S8D). In fact, as said before, according to sulphate isotopic composition, PZ-1 did not reach significant sulphate reducing conditions (Fig. 3). This was most likely caused by the consumption and absence of electron donor from t_{86} onwards or fast entrance of oxidizing groundwater. In contrast, possibly due to the combination of preferential flow paths and the influence of external active remediation systems (P&T and DPE) on the groundwater flow direction, certain amounts of organic acids arrived to wells PZ-6 and MW-6 (Figs. S9C and S10C), which were

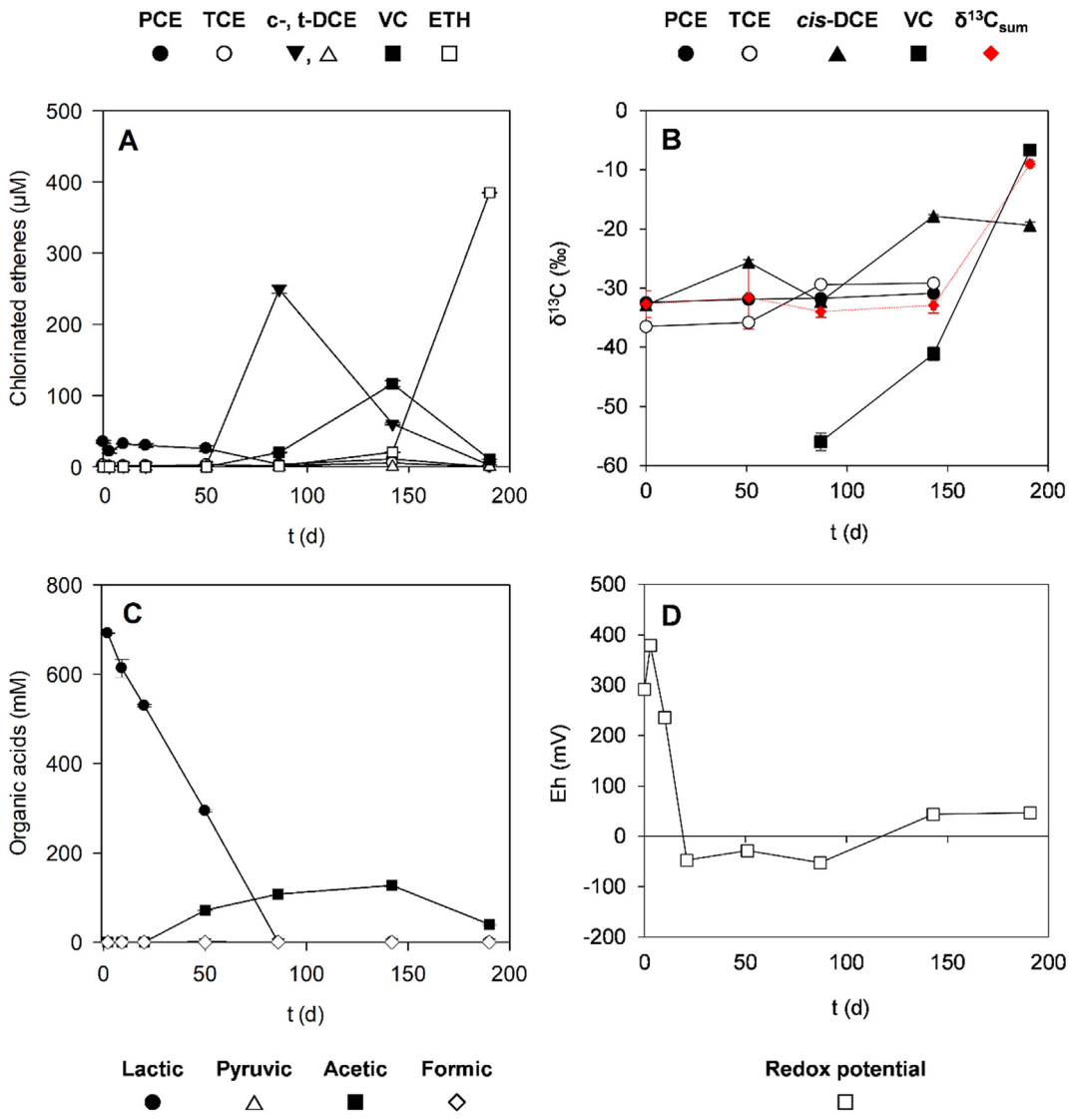

Fig. 4. Time-course of monitored parameters at well PZ-2 during the *in-situ* pilot test: (A) concentration of CEs; (B) carbon isotopic composition and balance; (C) concentration of organic acids, and (D) redox potential (Eh). Data presented is an average of each sampling event and includes error bars showing the one standard deviation (1σ) for duplicate measurements.

the farthest from PZ-2. Their Eh decreased much more progressively after t_{50}, and remained negative until t_{190}, allowing sulphate reducing conditions and further degradation to VC (Figs. S9D and S10D).

3.2.4. Impact of the in-situ pilot test in wells outside the direct radius of influence

Lactate and acetate were not detected in wells PZ-3, PZ-22, and Prof.D (Figures S11C, S12C and S13C). Accordingly, Eh did not reach negative values in any of them (Figures S11D, S12D and S13D), not allowing to prove a direct effect of the ERD pilot test. In well PZ-3, Eh decreased to +60 mV at t_{86} but it rebounded to initial conditions at t_{190} (Fig. S11D). Curiously, CEs concentrations decreased globally in PZ-3 and PZ-22, but PCE molar fraction increased in respect to its daughter products, which could indicate a solubilization and dilution of the PCE adsorbed to the soil due to the injected volume (Fig. S14). Therefore, the ^{13}C enrichments observed for TCE and *cis*-DCE in PZ-3 (by +11.5‰ and +8.1‰, respectively, Fig. S11) could be attributed to reductive dechlorination in the well or, most probably, associated to the dispersion from upstream contaminants (Fig. 1). In wells PZ-22 and Prof.D, changes in CEs concentrations (Figs. S12A and S13A) were not associated to significant shifts in ^{13}C values (Figs. S12B and S13B), confirming this dilution effect.

3.2.5. Changes in the native microbial community induced by the in-situ pilot test

The effect of lactate injection on the microbial community of the aquifer was investigated by high-throughput sequencing of the 16S rRNA region of selected groundwater samples. PZ-2, PZ-1 and PZ-22 at t_{-1} and t_{142} were chosen based on the results obtained in the pilot test, as they represented three different scenarios: i) PCE-to-ETH reaction at the injection well (PZ-2), ii) *cis*-DCE stall (PZ-1), and iii) a well not directly impacted by the injection of lactate (PZ-22). In PZ-2, the most abundant phyla at t_{-1} were *Proteobacteria* (58%), *Planctomycetes* (11%), *Bacteroidetes* (6%), *Verrucomicrobia* (6%), *Chlamydiae* (4%), *Actinobacteria* (4%), and *Acidobacteria* (2%), whereas at t_{142}, the community shifted to *Firmicutes* (67%), *Bacteroidetes* (14%), *Proteobacteria* (14%), and *Tenericutes* (2%) (Fig. 6, Table S4). Within *Firmicutes*, bacteria from the family *Veillonellaceae* (26%), and *Erysipelotrichaceae* (9%) were the most abundant; and

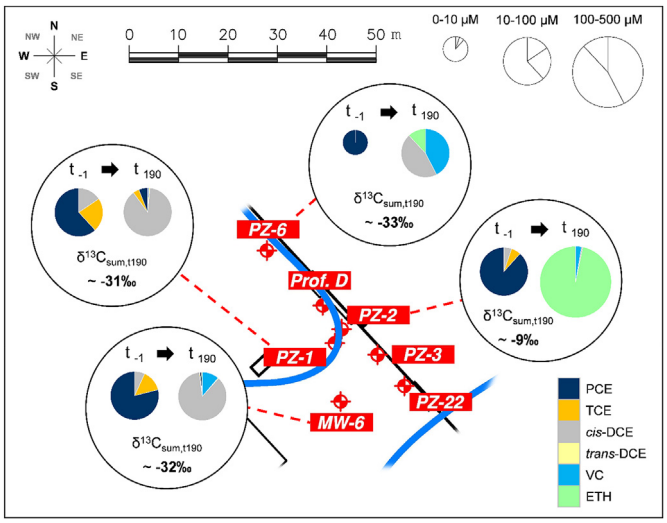

Fig. 5. Location of the lactate injection well (PZ-2) and the monitoring wells of the *in-situ* ERD pilot test where the influence of the biostimulation was proved along 190 days, indicating the molar fraction shift of CEs + ETH and the final carbon isotopic mass balance ($\delta^{13}C_{sum,t190}$). The size of the pie charts is related to the total concentration of CEs + ETH in each well and sampling time. For more detailed results, see Figs. 4, S8, S9 and S10.

the same occurred for the genus *Desulfovibrio* (3%), from the *Proteobacteria* phylum (data not shown). The microbial composition after the injection of lactate was dominated by fermenting bacteria that were probably induced by the injection of lactate (Fennell et al., 1997; He et al., 2007; Tegtmeier et al., 2016). In contrast, the abundance of the *Firmicutes* phylum was very limited in well PZ-1 (abundance of 4% at t_{142}) and almost insignificant in well PZ-22, which agrees with the chemical and isotopic results discussed before.

3.3. Isotopic evaluation of the full-scale ERD with lactate

After the *in-situ* ERD pilot test, which finished in June 2017, a full-scale ERD with Lactate-2 was implemented on August 2017. After one year of full-scale treatment (from August 2017 to September 2018), an isotopic mass balance of CEs was calculated from 6 selected monitoring wells (PZ-3, PZ-5, PZ-22, MW-3, MW-6, MW-7, Fig. 1) to evaluate the extent and success of the full-scale ERD. Results revealed that PCE and TCE were completely depleted in 5 out of the 6 monitoring wells and VC and ETH were the major end products (Table 1). Originally, $\delta^{13}C_{sum}$ at the site was, in average, of -30 ± 2‰, which responded to the original $\delta^{13}C$ value of PCE (Blázquez-Pallí et al., 2019). After one year of full-scale ERD, the $\delta^{13}C_{sum}$ values in those 5 wells were enriched (ranging from -23.2 ± 0.5‰ to -13 ± 1‰) with respect to the initial value (Table 1). This trend in $\delta^{13}C_{sum}$ of becoming more positive was also observed in well PZ-2 during the *in-situ* pilot test and responds to ETH production. In the case of MW-7, the $\delta^{13}C_{sum}$ was already different from the rest of the wells in the characterization campaign (May 2016) (Blázquez-Pallí et al., 2019), but biodegradation up to VC has been also observed after the full-scale (Table 1). Therefore, these results confirmed that the reductive dechlorination of CEs was occurring across the site, albeit at different extent in each well.

4. Conclusions

The present study aimed at validating a multidisciplinary methodology to assess and monitor biodegradation of CEs at the field scale. In this work, hydrochemical, isotopic and microbiological data from the field was examined together with aquifer-derived

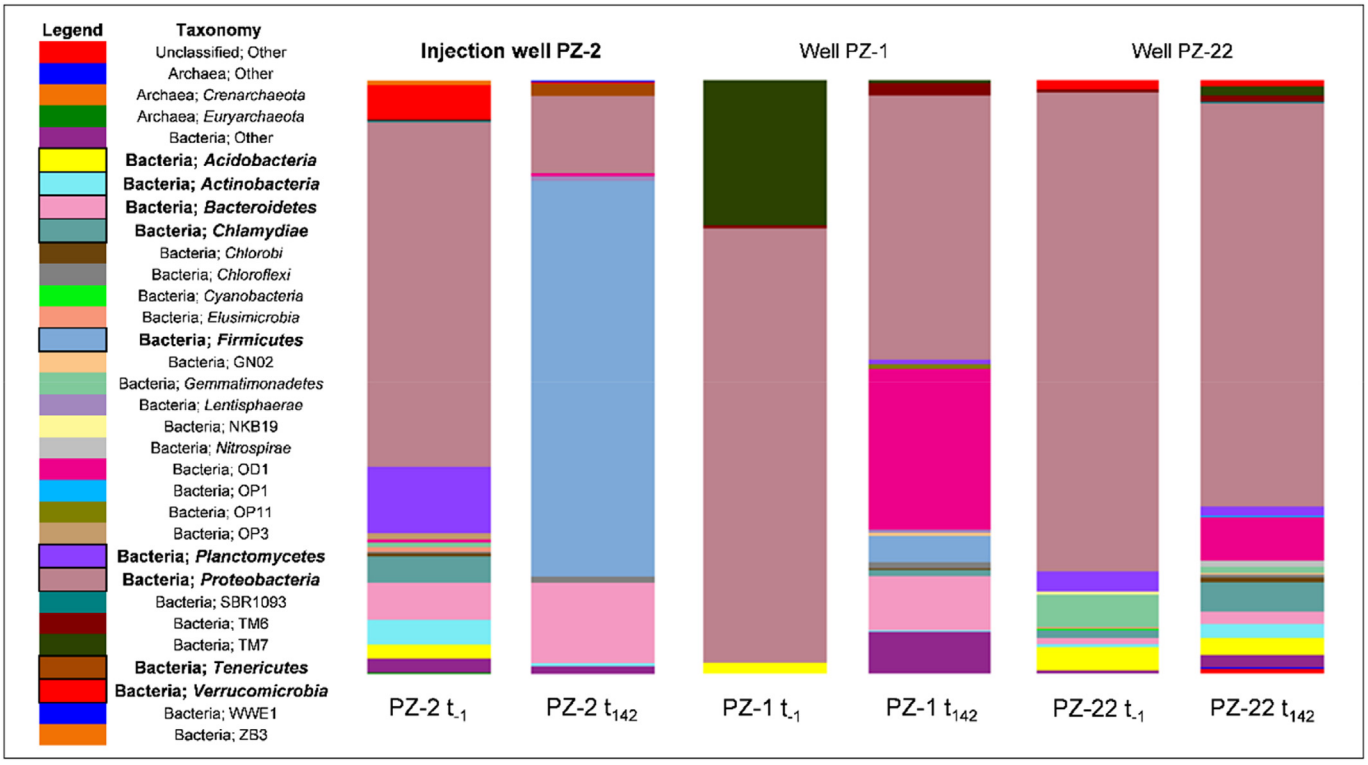

Fig. 6. 16S rRNA high-throughput sequencing results at the phylum level for wells PZ-2, PZ-1, and PZ-22 before lactate injection (t_{-1}) and after injection (t_{142}). Detailed abundance (in %) is presented in Table S4. Phyla in bold are the most abundant in PZ-2 (either at t_{-1} or t_{142}).

Table 1
Molar concentrations (in μM), $\delta^{13}C$ (in ‰) of contaminants and isotopic mass balance ($\delta^{13}C_{sum}$) in September 2018, after one year of full-scale ERD with lactate at the site. Comparison with the results obtained in the field characterization before any biostimulation treatment (either May 2016 or t_{-1}).

Well	Campaign	PCE (μM)	TCE (μM)	*cis*-DCE (μM)	VC (μM)	ETH (μM)
PZ-3	t_{-1}	10.4 ± 0.5	3.6 ± 0.1	10.5 ± 0.4	<0.3	<0.2
	Sept. 2018	<0.2	<0.2	0.6 ± 0.1	<0.3	0.2 ± 0.1
PZ-5	May 2016	77.1	2.6	1.9	<0.3	<0.2
	Sept. 2018	<0.2	<0.2	3.1 ± 0.1	10.6 ± 0.8	34 ± 3
PZ-22	t_{-1}	16 ± 2	0.42 ± 0.01	0.8 ± 0.2	<0.3	<0.2
	Sept. 2018	<0.2	<0.2	4.7 ± 0.1	0.7 ± 0.1	1.02 ± 0.01
MW-3	May 2016	29 ± 5	0.49 ± 0.07	0.56 ± 0.01	<0.3	<0.2
	Sept. 2018	<0.2	<0.2	0.6 ± 0.1	29 ± 1	24.8 ± 0.3
MW-6	t_{-1}	52 ± 5	9.4 ± 0.8	4.5 ± 0.4	<0.3	<0.2
	Sept. 2018	<0.2	<0.2	<0.3	<0.3	0.9 ± 0.1
MW-7	May 2016	61 ± 14	0.6 ± 0.1	0.56 ± 0.01	<0.3	<0.2
	Sept. 2018	1.7 ± 0.1	0.8 ± 0.1	15.9 ± 0.3	56 ± 3	17 ± 2

Well	Campaign	PCE $\delta^{13}C$ (‰)	TCE $\delta^{13}C$ (‰)	*cis*-DCE $\delta^{13}C$ (‰)	VC $\delta^{13}C$ (‰)	$\delta^{13}C_{sum}$ (‰)
PZ-3	t_{-1}	−31.7 ± 0.5	−29.1 ± 0.5	−29.7 ± 0.5	n.d.	−30 ± 1
	Sept. 2018	n.d.	n.d.	−16.7 ± 0.4	n.d.	−16.7 ± 0.4
PZ-5	May 2016	−29.8 ± 0.4	−29.7 ± 0.5	−33.0 ± 0.7	n.d.	−29.8 ± 0.4
	Sept. 2018	n.d.	n.d.	−14.3 ± 0.4	−23.5 ± 0.6	−21 ± 2
PZ-22	t_{-1}	−32.9 ± 0.5	−26.3 ± 0.6	−22.5 ± 0.3	n.d.	−32 ± 5
	Sept. 2018	n.d.	n.d.	−23.2 ± 0.5	n.d.	−23.2 ± 0.5
MW-3	May 2016	−31.0 ± 0.7	n.d.	n.d.	n.d.	−31.0 ± 0.7
	Sept. 2018	n.d.	n.d.	−10.4 ± 0.6	−12.8 ± 0.3	−13 ± 1
MW-6	t_{-1}	−31.2 ± 0.4	−34.5 ± 0.6	−32.1 ± 0.5	n.d.	−32 ± 3
	Sept. 2018	n.d.	n.d.	n.d.	n.d.	n.a.
MW-7	May 2016	−26.4 ± 0.6	n.d.	n.d.	n.d.	−26.4 ± 0.6
	Sept. 2018	−27.1 ± 0.4	−25.1 ± 0.4	−23.0 ± 0.6	−25.2 ± 0.6	−25 ± 2

May 2016 campaign: results from the field site characterization reported in Blázquez-Pallí et al. (2019). n.d.: not detected due to concentrations being below the limit of quantification, n.a.: not applicable.

laboratory microcosms to get an insight into the idiosyncrasies of the aquifer. The first part of this study focused on the diagnosis of the *in-situ* biodegradation potential of the site for full reductive dechlorination of CEs. The results obtained provided evidence that the stall at *cis*-DCE and VC was due to the lack of electron donors. Afterwards, the injection of lactate in a monitoring well evidenced that full reductive dechlorination to ETH was achieved within 190 days, and that the reaction followed a different pace in the surrounding monitoring wells. Therefore, the hydrodynamic characteristics of the aquifer possibly dominated the distribution of electron donor, hence, affecting the outcome of the biodegradation reaction in the studied surrounding wells. The methodology proposed here can be easily integrated as a tool in the early stages of site investigation to decide which bioremediation strategy is more suitable according to the specific characteristics of the aquifer. Moreover, it can reduce the uncertainties regarding the ongoing processes that are occurring in groundwater systems. Finally, the initial isotopic characterization of the site allowed for applying isotope-mass balance calculations to unequivocally demonstrate ETH generation after the full-scale enhanced reductive dechlorination via lactate injection. This stable isotope-based technique can overcome the difficulties related to the traditional mass balance approaches which are often hindered by natural processes (e.g. dilution, sorption, volatilization).

Declaration of competing interest

The authors declare that they have no known competing financial interests or personal relationships that could have appeared to influence the work reported in this paper.

Acknowledgements

This research has been supported by *Agencia Estatal de Investigación* (CTM2016-75587-C2-1-R, CGL2014-57215-C4-1-R and CGL2017-87216-C4-1-R projects) and co-financed by the European Union through the European Regional Development Fund (ERDF). This work was also partly supported by *Generalitat de Catalunya* through the consolidate research groups (2017-SGR-14 and 2017SGR-1733) and the Industrial Doctorate grant (2015-DI-064) of N. Blázquez-Pallí. M. Rosell acknowledges a *Ramón y Cajal* contract (RYC-2012-11920) from MINECO. The *Departament d'Enginyeria Química, Biològica i Ambiental* of *Universitat Autònoma de Barcelona* is a member of *Xarxa de Referència en Biotecnologia de la Generalitat de Catalunya*. We thank Dr. Ivonne Nijenhuis for providing *Dehalococcoides mccartyi* BTF08, Dr. Cristina Domènech for the geochemical modelling advice, David Fernández-Verdejo for his contribution in the laboratory work, and CCiT-UB and Dr. Roger Puig for excellent technical assistance.

Appendix A. Supplementary data

Supplementary data to this article can be found online at https://doi.org/10.1016/j.watres.2019.115106.

References

Adrian, L., Löffler, F.E., 2016. Organohalide-Respiring Bacteria, Organohalide-Respiring Bacteria. Springer Berlin Heidelberg, Berlin, Heidelberg. https://doi.org/10.1007/978-3-662-49875-0.

Aelion, C.M., Höhener, P., Hunkeler, D., Aravena, R., 2009. Environmental Isotopes in Bioremediation and Biodegradation. CRC Press, Boca Raton. https://doi.org/10.1159/000076616.

Aeppli, C., Hofstetter, T.B., Amaral, H.I.F., Kipfer, R., Schwarzenbach, R.P., Berg, M., 2010. Quantifying in situ transformation rates of chlorinated ethenes by combining compound-specific stable isotope analysis, groundwater dating, and carbon isotope mass balances. Environ. Sci. Technol. 44, 3705–3711. https://doi.org/10.1021/es903895b.

Antler, G., Turchyn, A. V, Rennie, V., Herut, B., Sivan, O., 2013. Coupled sulfur and oxygen isotope insight into bacterial sulfate reduction in the natural environment. Geochem. Cosmochim. Acta 118, 98–117. https://doi.org/10.1016/j.gca.2013.05.005.

Atashgahi, S., Lu, Y., Smidt, H., 2016. Overview of known organohalide-respiring bacteria-phylogenetic diversity and environmental distribution. In: Adrian, L.,

Löffler, F.E. (Eds.), Organohalide-Respiring Bacteria. Springer Berlin Heidelberg, Berlin, Heidelberg, pp. 63–105. https://doi.org/10.1007/978-3-662-49875-0_5.
ATSDR, 2017. Substance priority list. https://www.atsdr.cdc.gov/SPL/index.html#2017spl [WWW Document], Agency Toxic Subst. Dis. Regist, accessed 4.17.19.
Blázquez-Pallí, N., Rosell, M., Varias, J., Bosch, M., Soler, A., Vicent, T., Marco-Urrea, E., 2019. Multi-method assessment of the intrinsic biodegradation potential of an aquifer contaminated with chlorinated ethenes at an industrial area in Barcelona (Spain). Environ. Pollut. 244, 165–173. https://doi.org/10.1016/j.envpol.2018.10.013.
Bradley, P.M., 2000. Microbial degradation of chloroethenes in groundwater systems. Hydrogeol. J. 8, 251–253. https://doi.org/10.1007/s100400050011.
Buchner, D., Behrens, S., Laskov, C., Haderlein, S.B., 2015. Resiliency of stable isotope fractionation (δ13C and δ37Cl) of trichloroethene to bacterial growth physiology and expression of key enzymes. Environ. Sci. Technol. 49, 13230–13237. https://doi.org/10.1021/acs.est.5b02918.
Cichocka, D., Imfeld, G., Richnow, H.H., Nijenhuis, I., 2008. Variability in microbial carbon isotope fractionation of tetra- and trichloroethene upon reductive dechlorination. Chemosphere 71, 639–648. https://doi.org/10.1016/j.chemosphere.2007.11.013.
Courbet, C., Rivière, A., Jeannottat, S., Rinaldi, S., Hunkeler, D., Bendjoudi, H., de Marsily, G., 2011. Complementing approaches to demonstrate chlorinated solvent biodegradation in a complex pollution plume: mass balance, PCR and compound-specific stable isotope analysis. J. Contam. Hydrol. 126, 315–329. https://doi.org/10.1016/j.jconhyd.2011.08.009.
Dogramaci, S., Herczeg, A., Schiff, S., Bone, Y., 2001. Controls on δ 34 S and δ 18 O of dissolved sulfate in aquifers of the Murray Basin, Australia and their use as indicators of flow processes. Appl. Geochem. 16, 475–488. https://doi.org/10.1016/S0883-2927(00)00052-4.
Dugat-Bony, E., Biderre-Petit, C., Jaziri, F., David, M.M., Denonfoux, J., Lyon, D.Y., Richard, J.-Y., Curvers, C., Boucher, D., Vogel, T.M., Peyretaillade, E., Peyret, P., 2012. In situ TCE degradation mediated by complex dehalorespiring communities during biostimulation processes. Microb. Biotechnol. 5, 642–653. https://doi.org/10.1111/j.1751-7915.2012.00339.x.
Ebert, K., Laskov, C., Behrens, S., Haderlein, S.B., 2010. Assessment of chlorinated ethenes biodegradation in an anaerobic aquifer by isotope analysis and microcosm studies. IAHS Publ. 342, 13–18.
Elsner, M., 2010. Stable isotope fractionation to investigate natural transformation mechanisms of organic contaminants: principles, prospects and limitations. J. Environ. Monit. 12, 2005–2031. https://doi.org/10.1039/c0em00277a.
European Commission, 2008. Directive 2008/105/EC of 16 December 2008 on environmental quality standards in the field of water policy. Off. J. Eur.Union. https://eur-lex.europa.eu/legal-content/EN/TXT/?uri=celex:32008L0105.
Fennell, D.E., Gossett, J.M., Zinder, S.H., 1997. Comparison of butyric acid, ethanol, lactic acid, and propionic acid as hydrogen donors for the reductive dechlorination of tetrachloroethene. Environ. Sci. Technol. 31, 918–926. https://doi.org/10.1021/es960756r.
He, J., Holmes, V.F., Lee, P.K.H., Alvarez-Cohen, L., 2007. Influence of vitamin B12 and cocultures on the growth of Dehalococcoides isolates in defined medium. Appl. Environ. Microbiol. 73, 2847–2853. https://doi.org/10.1128/AEM.02574-06.
Herlemann, D.P.R., Labrenz, M., Jürgens, K., Bertilsson, S., Waniek, J.J., Andersson, A.F., 2011. Transitions in bacterial communities along the 2000 km salinity gradient of the Baltic Sea. ISME J. 5, 1571–1579. https://doi.org/10.1038/ismej.2011.41.
Hermon, L., Denonfoux, J., Hellal, J., Joulian, C., Ferreira, S., Vuilleumier, S., Imfeld, G., 2018. Dichloromethane biodegradation in multi-contaminated groundwater: insights from biomolecular and compound-specific isotope analyses. Water Res. 142, 217–226. https://doi.org/10.1016/j.watres.2018.05.057.
Hermon, L., Hellal, J., Denonfoux, J., Vuilleumier, S., Imfeld, G., Urien, C., Ferreira, S., Joulian, C., 2019. Functional genes and bacterial communities during organohalide respiration of chloroethenes in microcosms of multi-contaminated groundwater. Front. Microbiol. 10, 89. https://doi.org/10.3389/fmicb.2019.00089.
Herrero, J., Puigserver, D., Nijenhuis, I., Kuntze, K., Carmona, J.M., 2019. Combined use of ISCR and biostimulation techniques in incomplete processes of reductive dehalogenation of chlorinated solvents. Sci. Total Environ. 648, 819–829. https://doi.org/10.1016/j.scitotenv.2018.08.184.
Hirschorn, S.K., Grostern, A., Lacrampe-Couloume, G., Edwards, E.A., MacKinnon, L., Repta, C., Major, D.W., Sherwood Lollar, B., 2007. Quantification of biotransformation of chlorinated hydrocarbons in a biostimulation study: added value via stable carbon isotope analysis. J. Contam. Hydrol. 94, 249–260. https://doi.org/10.1016/j.jconhyd.2007.07.001.
Hunkeler, D., Aravena, R., Butler, B.J., 1999. Monitoring microbial dechlorination of tetrachloroethene (PCE) in groundwater using compound-specific stable carbon isotope ratios: microcosm and field studies. Environ. Sci. Technol. 33, 2733–2738. https://doi.org/10.1021/es981282u.
Hunkeler, D., Meckenstock, R.U., Lollar, B.S., Schmidt, T.C., Wilson, J.T., 2008. A Guide for Assessing Biodegradation and Source Identification of Organic Ground Water Contaminants Using Compound Specific Isotope Analysis (CSIA). U.S. Environmental Protection Agency, Washington, D.C. EPA/600/R-08/148.
Im, W.T., Kim, S.H., Kim, M.K., Ten, L.N., Lee, S.T., 2006. Pleomorphomonas koreensis sp. nov., a nitrogen-fixing species in the order Rhizobiales. Int. J. Syst. Evol. Microbiol. 56, 1663–1666. https://doi.org/10.1099/ijs.0.63499-0.
Klindworth, A., Pruesse, E., Schweer, T., Peplies, J., Quast, C., Horn, M., Glöckner, F.O., 2013. Evaluation of general 16S ribosomal RNA gene PCR primers for classical and next-generation sequencing-based diversity studies. Nucleic Acids Res. 41 e1–e1. https://doi.org/10.1093/nar/gks808.
Kuder, T., Van Breukelen, B.M., Vanderford, M., Philp, P., 2013. 3D-CSIA: carbon, chlorine, and hydrogen isotope fractionation in transformation of TCE to ethene by a dehalococcoides culture. Environ. Sci. Technol. 47, 9668–9677. https://doi.org/10.1021/es400463p.
Lee, J., Im, J., Kim, U., Löffler, F.E., 2016. A data mining approach to predict in situ detoxification potential of chlorinated ethenes. Environ. Sci. Technol. 50, 5181–5188. https://doi.org/10.1021/acs.est.5b05090.
Leeson, A., Beevar, E., Henry, B.M., Fortenberry, J., Coyle, C., Parsons, Corp, 2004. Principles and Practices of Enhanced Anaerobic Bioremediation of Chlorinated Solvents. Port Hueneme, California. ESTCP CU 0125.
Leys, D., Adrian, L., Smidt, H., 2013. Organohalide respiration: microbes breathing chlorinated molecules. Philos. Trans. R. Soc. Lond. B Biol. Sci. 368, 20120316. https://doi.org/10.1098/rstb.2012.0316.
Löffler, F.E., Sanford, R.A., Ritalahti, K.M., 2005. Enrichment, cultivation, and detection of reductively dechlorinating bacteria. Methods Enzymol. 397, 77–111. https://doi.org/10.1016/S0076-6879(05)97005-5.
Lu, X., Wilson, J.T., Kampbell, D.H., 2009. Comparison of an assay for Dehalococcoides DNA and a microcosm study in predicting reductive dechlorination of chlorinated ethenes in the field. Environ. Pollut. 157, 809–815. https://doi.org/10.1016/j.envpol.2008.11.015.
Madhaiyan, M., Jin, T.Y., Roy, J.J., Kim, S.-J., Weon, H.-Y., Kwon, S.-W., Ji, L., 2013. Pleomorphomonas diazotrophica sp. nov., an endophytic N-fixing bacterium isolated from root tissue of Jatropha curcas L. Int. J. Syst. Evol. Microbiol. 63, 2477–2483. https://doi.org/10.1099/ijs.0.044461-0.
Martín-González, L., Mortan, S.H., Rosell, M., Parladé, E., Martínez-Alonso, M., Gaju, N., Caminal, G., Adrian, L., Marco-Urrea, E., 2015. Stable carbon isotope fractionation during 1,2-dichloropropane-to-propene transformation by an enrichment culture containing Dehalogenimonas strains and a dcpA gene. Environ. Sci. Technol. 49, 8666–8674. https://doi.org/10.1021/acs.est.5b00929.
Matteucci, F., Ercole, C., Del Gallo, M., 2015. A study of chlorinated solvent contamination of the aquifers of an industrial area in central Italy: a possibility of bioremediation. Front. Microbiol. 6, 1–10. https://doi.org/10.3389/fmicb.2015.00924.
Mizutani, Y., Rafter, T.A., 1973. Isotopic behaviour of sulphate oxygen in the bacterial reduction of sulphate. Geochem. J. 6, 183–191. https://doi.org/10.2343/geochemj.6.183.
Mortan, S.H., Martín-González, L., Vicent, T., Caminal, G., Nijenhuis, I., Adrian, L., Marco-Urrea, E., 2017. Detoxification of 1,1,2-trichloroethane to ethene in a bioreactor co-culture of Dehalogenimonas and Dehalococcoides mccartyi strains. J. Hazard Mater. 331, 218–225. https://doi.org/10.1016/j.jhazmat.2017.02.043.
Nijenhuis, I., Nikolausz, M., Köth, A., Felföldi, T., Weiss, H., Drangmeister, J., Großmann, J., Kästner, M., Richnow, H.H., 2007. Assessment of the natural attenuation of chlorinated ethenes in an anaerobic contaminated aquifer in the Bitterfeld/Wolfen area using stable isotope techniques, microcosm studies and molecular biomarkers. Chemosphere 67, 300–311. https://doi.org/10.1016/j.chemosphere.2006.09.084.
Otero, N., Soler, A., Canals, À., 2008. Controls of δ34S and δ18O in dissolved sulphate: learning from a detailed survey in the Llobregat River (Spain). Appl. Geochem. 23, 1166–1185. https://doi.org/10.1016/j.apgeochem.2007.11.009.
Palau, J., Marchesi, M., Chambon, J.C.C., Aravena, R., Canals, À., Binning, P.J., Bjerg, P.L., Otero, N., Soler, A., 2014. Multi-isotope (carbon and chlorine) analysis for fingerprinting and site characterization at a fractured bedrock aquifer contaminated by chlorinated ethenes. Sci. Total Environ. 475, 61–70. https://doi.org/10.1016/j.scitotenv.2013.12.059.
Puigdomènech, I., 2010. MEDUSA (Make Equilibrium Diagrams Using Sophisticated Algorithms) Windows Interface to the MS-DOS Versions of INPUT, SED and PREDOM (FORTRAN Programs Drawing Chemical Equilibrium Diagrams) Vers. R. Inst. Technol. Stock. Sweden, 6 Dec 2010.
Rodríguez-Fernández, D., Torrentó, C., Palau, J., Marchesi, M., Soler, A., Hunkeler, D., Domènech, C., Rosell, M., 2018. Unravelling long-term source removal effects and chlorinated methanes natural attenuation processes by C and Cl stable isotopic patterns at a complex field site. Sci. Total Environ. 645, 286–296. https://doi.org/10.1016/j.scitotenv.2018.07.130.
Sanford, R.A., Chowdhary, J., Löffler, F.E., 2016. Organohalide-respiring deltaproteobacteria. In: Adrian, L., Löffler, F.E. (Eds.), Organohalide-Respiring Bacteria. Springer Berlin Heidelberg, Berlin, Heidelberg, pp. 235–258. https://doi.org/10.1007/978-3-662-49875-0_11.
Scheutz, C., Durant, N.D., Dennis, P., Hansen, M.H., Jørgensen, T., Jakobsen, R., Cox, E.e., Bjerg, P.L., 2008. Concurrent ethene generation and growth of Dehalococcoides containing vinyl chloride reductive dehalogenase genes during an enhanced reductive dechlorination field demonstration. Environ. Sci. Technol. 42, 9302–9309. https://doi.org/10.1021/es800764t.
Sharak Genthner, B.R., Friedman, S.D., Devereux, R., 1997. Reclassification of Desulfovibrio desulfuricans Norway 4 as Desulfomicrobium norvegicum comb. nov. and confirmation of Desulfomicrobium escambiense (corrig). Int. J. Syst. Bacteriol. 47, 889–892.
Sharak Genthner, B.R., Mundfrom, G., Devereux, R., 1994. Characterization of Desulfomicrobium escambium sp. nov. and proposal to assign Desulfovibrio desulfuricans strain Norway 4 to the genus Desulfomicrobium. Arch. Microbiol. 161, 215–219. https://doi.org/10.1007/BF00248695.
Sherwood Lollar, Barbara, Hirschorn, S.K., Chartrand, M.M.G., Lacrampe-Couloume, G., Sherwood Lollar, B., 2007. An approach for assessing total

instrumental uncertainty in compound-specific carbon isotope analysis: implications for environmental remediation studies. Anal. Chem. 79, 3469–3475. https://doi.org/10.1021/ac062299v.

Slater, G.F., Sherwood Lollar, Barbara, Sleep, B.E., Edwards, E.A., Sherwood Lollar, B., 2001. Variability in carbon isotopic fractionation during biodegradation of chlorinated ethenes: implications for field applications. Environ. Sci. Technol. 35, 901–907. https://doi.org/10.1021/es001583f.

Song, D.L., Conrad, M.E., Sorenson, K.S., Alvarez-Cohen, L., 2002. Stable carbon isotope fractionation during enhanced in situ bioremediation of trichloroethene. Environ. Sci. Technol. 36, 2262–2268. https://doi.org/10.1021/es011162d.

Stroo, H.F., Ward, C.H., 2010. In: In Situ Remediation of Chlorinated Solvent Plumes, 1st Ed, SERDP/ESTCP Environmental Remediation Technology. Springer New York, New York, NY. https://doi.org/10.1007/978-1-4419-1401-9.

Tarnawski, S.-E., Rossi, P., Brennerova, M.V., Stavelova, M., Holliger, C., 2016. Validation of an integrative methodology to assess and monitor reductive dechlorination of chlorinated ethenes in contaminated aquifers. Front. Environ. Sci. 4, 1–16. https://doi.org/10.3389/fenvs.2016.00007.

Tegtmeier, D., Riese, C., Geissinger, O., Radek, R., Brune, A., 2016. Breznakia blatticola gen. nov. sp. nov. and Breznakia pachnodae sp. nov., two fermenting bacteria isolated from insect guts, and emended description of the family Erysipelotrichaceae. Syst. Appl. Microbiol. 39, 319–329. https://doi.org/10.1016/j.syapm.2016.05.003.

Wu, S., Jeschke, C., Dong, R., Paschke, H., Kuschk, P., Knöller, K., 2011. Sulfur transformations in pilot-scale constructed wetland treating high sulfate-containing contaminated groundwater: a stable isotope assessment. Water Res. 45, 6688–6698. https://doi.org/10.1016/j.watres.2011.10.008.

Xie, C.H., Yokota, A., 2005. Pleomorphomonas oryzae gen. nov., sp. nov., a nitrogen-fixing bacterium isolated from paddy soil of Oryza sativa. Int. J. Syst. Evol. Microbiol. 55, 1233–1237. https://doi.org/10.1099/ijs.0.63406-0.

Yang, Y., Cápiro, N.L., Marcet, T.F., Yan, J., Pennell, K.D., Löffler, F.E., 2017a. Organohalide respiration with chlorinated ethenes under low pH conditions. Environ. Sci. Technol. 51, 8579–8588. https://doi.org/10.1021/acs.est.7b01510.

Yang, Y., Higgins, S.A., Yan, J., Şimşir, B., Chourey, K., Iyer, R., Hettich, R.L., Baldwin, B.R., Ogles, D.M., Löffler, F.E., 2017b. Grape pomace compost harbors organohalide-respiring Dehalogenimonas species with novel reductive dehalogenase genes. ISME J. 11, 2767–2780. https://doi.org/10.1038/ismej.2017.127.

Yu, R., Andrachek, R.G., Lehmicke, L.G., Freedman, D.L., 2018. Remediation of chlorinated ethenes in fractured sandstone by natural and enhanced biotic and abiotic processes: a crushed rock microcosm study. Sci. Total Environ. 626, 497–506. https://doi.org/10.1016/j.scitotenv.2018.01.064.